

# Wind-Optimal Routing in the National Airspace System

Kee Palopo\* and Robert D. Windhorst†

NASA Ames Research Center, Moffett Field, California 94035

and

Salman Suharwardy‡ and Hak-Tae Lee§

University Affiliated Research Center, Moffett Field, California 94035

DOI: 10.2514/1.C000208

**A study analyzing the economic cost and benefit impacts of different flight routing methods in the National Airspace System is presented. It compares wind-optimal routes and filed flight routes for 365 days of traffic, from 2005 to 2007, in class A airspace. Routing differences are measured by flight time, fuel burn, sector loading, conflict counts, and airport arrival rates. From the results, wind-optimal routes exhibit an average per-flight time saving of 2.7 min and an average fuel saving of 210 lb, compared to filed flight routes. In addition, the airport arrival rates at the top 73 U.S. domestic airports do not show notable differences between wind-optimal routing and filed flight routing. The study shows an average of 29% fewer conflicts. Finally, wind-optimal routes have, at most, one high-altitude sector with increased sector workload than filed flight routes at any time instance.**

## Nomenclature

|            |   |                    |
|------------|---|--------------------|
| $D$        | = | distance, n mile   |
| $d$        | = | distance           |
| $T$        | = | time, h            |
| $V$        | = | speed, kt          |
| $\Delta T$ | = | time difference, h |

### Subscripts

|      |   |                                |
|------|---|--------------------------------|
| $d$  | = | distance                       |
| FFR  | = | filed flight route             |
| NOWR | = | neighboring optimal wind route |
| $w$  | = | wind                           |

## I. Introduction

**T**ODAY, most flight segments still must use the air traffic controller specified routes such as jet routes, airways, and very-high-frequency omnidirectional radio range waypoints, instead of flying user-preferred, optimal routes, which airlines have been capable of flying for decades. This is done for safety. Therefore, from an air traffic controller perspective, flying optimal routes in the continental U.S. airspace could only be allowed if these routes do not increase air traffic controller workload that may lead to safety issues. This is unlike flights in the Pacific, where near-wind-optimal routes are flown.

Numerous earlier studies looked at the benefits and costs of flight routings similar to those presented in this paper [1–7]. In [8], a cost and benefit study on proposed free flight, represented and approximated by great-circle flight plan routing, was performed. The

study found reduced number of conflicts in en route flight segments and found potential aggregate fuel savings. In [1], it was shown that significant cost savings can be achieved without adversely impacting the traffic management functions. In [2], fuel saving due to National Airspace System modernization was estimated by simulation models and extrapolation to the future. In [3], it was asserted that free flight would save flight times and fuel consumption and would save billions of dollars annually. In [4] the benefits of wind-optimal routing in the central east Pacific region were evaluated. The study found an average time and distance savings of 9.9 min and 36 n mile per flight, respectively. In [5], the conflict rates produced by great-circle routes and those used today were calculated. Great-circle routes had significantly fewer conflicts. In [9], a wind-optimal routing algorithm using neighboring optimal control technique was described. In [6], a relationship of air traffic density and conflicts in terms of wind-optimal routing was described. In [7], an economic and safety benefits comparison study was performed on user-filed, great-circle, and wind-optimal flight routes, using a one-day traffic demand set of 8 March 2007. The time and fuel savings that day amounted to 1.3 and 1.4%, respectively. The sector loading was qualitatively determined to be equivalent and the first-loss-of-separation conflict pair count was around 50% lower for the wind-optimal routing. The study found that wind-optimal routing has potential positive economic benefits without sacrificing safety, albeit based on a single day of data. Reference [7] and other previous studies' results were limited to a small number of days.

The follow-on study presented in this paper also compares the economic and workload impacts of flying wind-optimal routes and flying user-filed routes, but with 365 days in the National Airspace System. The associated traffic demand and wind data are from 2005 through 2007. This large, annual data set is expected to provide representative distributions of flights in the National Airspace System and statistically significant results. As a main contribution, this extended data set allows an insight into the variability of economic and safety benefits of flight routings in terms of their upper bound, an insight into some flights not flying more optimal routes, and an insight into portions of airspace with high complexity in the National Airspace System. In addition to flight time, fuel burn, sector loading, and number of conflicts metrics, this study also examines airport arrival rates as an additional workload factor. The study uses the same NASA Ames Research Center's Airspace Concept Evaluation System simulation tool described in [10].

The rest of the paper presents wind-optimal routes and user-filed routes in the next section, Routes, which is followed by the metrics used in the study. The Approach section describes the study's methodology, after which the results of the study are presented. The Conclusions include implications of using wind-optimal routes and

Presented as Paper 2009-6993 at the 9th AIAA Aviation Technology, Integration, and Operations Conference, Hilton Head, CA, 21–23 September 2009; received 2 December 2009; revision received 10 February 2010; accepted for publication 11 February 2010. This material is declared a work of the U.S. Government and is not subject to copyright protection in the United States. Copies of this paper may be made for personal or internal use, on condition that the copier pay the \$10.00 per-copy fee to the Copyright Clearance Center, Inc., 222 Rosewood Drive, Danvers, MA 01923; include the code 0021-8669/10 and \$10.00 in correspondence with the CCC.

\*Aerospace Engineer, Aerospace Systems Modeling and Optimization Branch, Mail Stop 210-15. Member AIAA.

†Chief, Aerospace Systems Modeling and Optimization Branch, Mail Stop 210-15. Senior Member AIAA.

‡Software Engineer, Aerospace Systems Modeling and Optimization Branch, Mail Stop 210-8. Member AIAA.

§Associate Scientist, Aerospace Systems Modeling and Optimization Branch, Mail Stop 210-8. Member AIAA (Corresponding Author).

summarize the major findings. Appendix A contains a derivation used in clarifying results.

## II. Routes

This section describes the two types of routes used in the study. A corresponding traffic demand set for each day is used for each type in the simulation.

### A. Filed Flight Route

The flight plans associated with the user-filed flight routes (FFRs) for 365 days come from the FAA's Enhanced Traffic Management System data, which contains user-filed flight plans that include route waypoints. As a user normally files and updates a flight plan for each flight, there are multiple entries per flight up to flight departure. Only the most recent flight plan before departure of each flight is used in this study. This flight plan is used in Airspace Concept Evaluation System (ACES) simulation and its resulting route serves as a baseline route for the comparison.

### B. Near-Optimal Wind Route

The flight plan associated with the near-optimal wind route (NOWR) contains a wind-optimized version of the FFR route with respect to flight time. Wind-optimal routes are generated offline for an airport pair using the algorithm described in [9] for the same 365 days. The algorithm assumes flights travel at constant altitude and airspeed. In this study, NOWRs are generated for flights that are flying between airports at least 500 n mile apart and are flying at a cruise altitude of flight level 180 (FL180) or 18,000 ft or higher. The former is to ensure each flight has a nonnegligible cruise segment with constant altitude and speed. The latter is to have a comparable class of airspace with previous studies. The inputs to the algorithm are the user-filed flight plan described above and a wind field. While FFRs are optimized and constrained on a number of criteria, including winds, crew costs, and fuel amount (see [11]), NOWRs are optimized on winds exclusively, with no other constraints. The performance of NOWRs varies under different wind fields and is expected to reflect seasonal wind patterns. These daily wind changes are explored in this study.

For simplicity, the NOWR algorithm is applied to flights from airport of origin to destination airport at cruise altitude, as described in [9]. The algorithm assumes constant airspeed and constant altitude (equal to cruise altitude), thus leading to some error in flight time estimates. This error accrues in the climb and descent segments, which are flown at different calibrated airspeeds and in a different wind field than the cruise altitude. The error is relatively small as already discussed in [7]. Additionally, the algorithm is only neighboring optimal, causing a relatively small number of NOWR cases to produce negative savings compared to their FFR counterparts, as discussed later.

## III. Metrics

Five metrics are used in the study. The first two metrics (flight time and fuel burn) allow researchers to look at economic impacts; the last three metrics (sector loading, conflicts, and airport arrival rates) help provide insight into workload impacts. The aim is to show benefits without incurring costs or at least no significant change.

### A. Flight Time

A flight time can be divided into surface time and airtime. The airtime consists of the time from takeoff to a departure fix, en route time, and the time from an arrival fix to touchdown. Furthermore, the en route time consists of the flight time from a departure fix to the top of climb, the cruise time, and the time from top of descent to an (initial) arrival fix. For simplicity, this paper compares the en route flight times for the daily demand of flights. Within the en route time portion, time saving is broken down into two components: that due to distance saving and that due to wind saving, as described in detail in

Appendix A. Flight time from flights below FL180 or flights shorter than 500 n mile is excluded from time-saving calculations.

### B. Fuel Burn

The fuel burn metric is the total fuel burn in pounds. This metric is correlated with the time metric. In ACES, fuel calculations for each flight are determined near the terminal areas and for its en route segment. Around terminals, fuel burn is derived using lookup tables, which contain fuel burn rate based on aircraft type. The fuel burn is proportional to the actual time spent in the terminal area. In the en route segment, fuel burn is modeled as a function of thrust, true airspeed, and altitude using the base aircraft data described in [12]. The mathematical relationship is detailed in [13]. Although a drill-down look at an individual aircraft's fuel burn can be performed, the results presented in this paper are aggregate. Fuel burn from flights below FL180 or flights shorter than 500 n mile are excluded from fuel-saving calculations.

### C. Sector Loading

The sector loading metric addresses congestion in various flight service provider areas. As with the next two metrics, sector loading affects manageability of the airspace in terms of human workload. It is measured in this study by looking at the 15 min peak count of flights in each sector for all 265 high-altitude sectors at FL180 and above. These peak counts are used to generate histograms of daily average number of sectors against peak counts and against sector monitor alert parameter (MAP) value, as described in the Results section. Aircraft counts exceeding the MAP values also indicates that in the real-world situation, delays will be incurred by the action of traffic flow management. Sector loading in the presence of weather is beyond the scope of this study.

### D. Conflicts

The conflicts metric is the number of conflict pairs. One flight in conflict with another at any instant of time counts as one conflict pair. A conflict is defined by a loss of separation, which occurs when aircraft are within 5 n mile laterally and 1000 ft vertically from each other. The vertical separation is based on the reduced-vertical-separation minimum (RVSM) introduced in January 2005 for the continental United States, for FL290 to FL410. In this study, conflicts are checked every 10 s for all flights at FL180 or above with the same vertical separation in RVSM. Similar to sector loading, the number of conflicts in a sector impacts the manageability of the airspace in terms of human workload.

### E. Airport Arrival Rate

The airport arrival rate metric measures the hourly flight arrivals at an airport. For the current study, runways are not distinguished, and the arrival rate is measured as the total number of aircraft landing in the airport per hour. In this study, the nation's top airports as defined by the Federal Aviation Administration Aviation System Performance Metrics (ASPM) are examined. There are currently 77 ASPM airports, but the four ASPM airports outside the continental United States are excluded from the analysis. This metric is used to gain insight into whether wind-optimal routing will increase the arrival loading, at least at these major airports.

## IV. Approach

The approach taken in this study consists of flight plan preparation, running simulations, output data postprocessing, and analysis. The approach begins with data preparation, including selecting flight plans and rapid-update-cycle nowcast wind data for a desired simulation date.

Figure 1 illustrates the overall simulation approach and is described below. As shown in Fig. 1, an ACES simulation is performed for each type of routing. The corresponding flight plan for each route type is fed into ACES for simulation. Simulation results

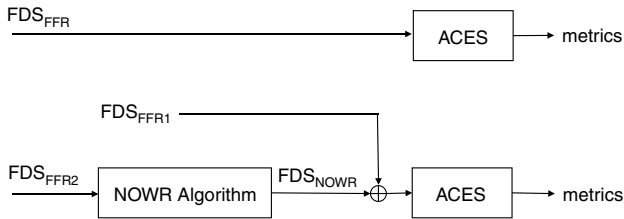


Fig. 1 Simulation approach.

that include the previously described metrics will be analyzed and presented.

The following description details how each flight plan for each day and each route type is prepared. For FFR, described in the Routes section, the corresponding input to ACES is FFR flight plan, and it is fed directly into ACES simulation. For NOWR, the same input flight plan is first split into two parts. One part is FFR2 and it has flight plans for airport-to-airport distances of 500 n mile or more and for cruise altitudes of 18,000 ft or more. Another part is FFR1 and it has the remaining flight plans. The former consists of 14,813 NOWR flights on average, or around 37% of average total of 40,493 flights. This part is fed into the NOWR algorithm to generate a wind-optimal version of the flight plans. The output of this algorithm is combined with FFR1 to become the flight plan for NOWR, which is then fed

into the ACES simulation. Although metrics are computed for all 40,493 flights, by splitting the data this way, only the common 14,813 flights are effectively compared while still maintaining a full-day effect of overall traffic. This is due to the equivalent results for the nonoptimized flights for both FFR and NOWR falling out of the comparison calculations. Figure 2 shows the overall three-year wind variation, which includes the one-year period data of interest. It shows the maximum wind speed for around 92% of days from 2005 through 2007. The remaining 8% of wind data is not available, and therefore its corresponding dates are not simulated. Of the available data, the average maximum wind speed is 151 kt, while the maximum wind speed ranges from 95 kt on 15 June 2005 to 215 kt on 15 January 2005 and 13 November 2006. Stronger maximum wind speeds are in the winter periods while weaker maximum wind speeds are in the summer periods. As a result, the benefits of wind-optimal routing are hypothesized to be larger in the winter months.

Finally, ACES' conflict resolution, air traffic control, and traffic flow management functionalities are disabled. These controls are disabled so the open-loop system response to changes in route structure can be studied under the heaviest workload conditions.

### V. Results

Results based on 365 days are presented below. The days are intended to span the calendar year 2007. However, some days from 2007 could not be simulated due to missing wind or flight-plan data,

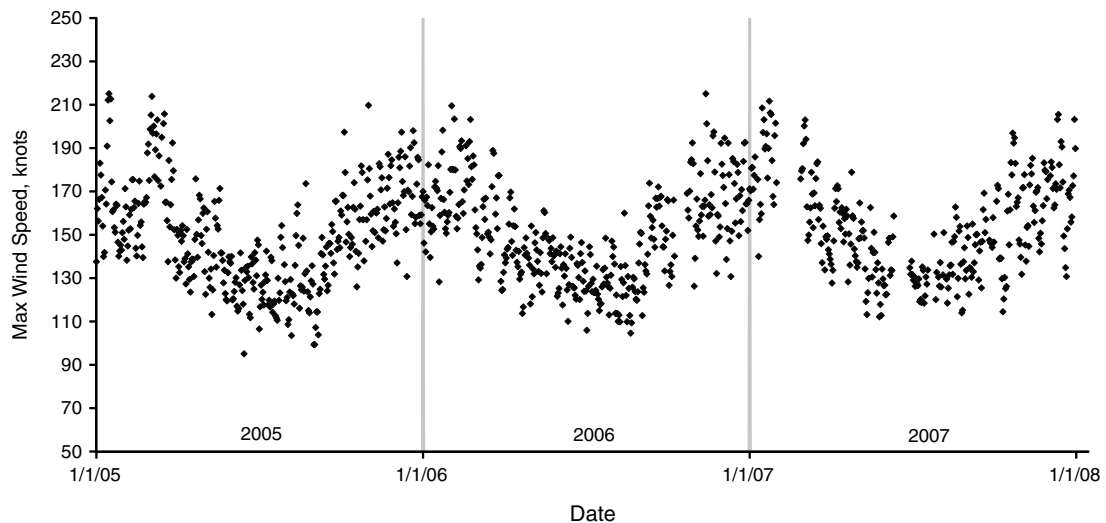


Fig. 2 Maximum wind speed, 2005–2007, in knots.

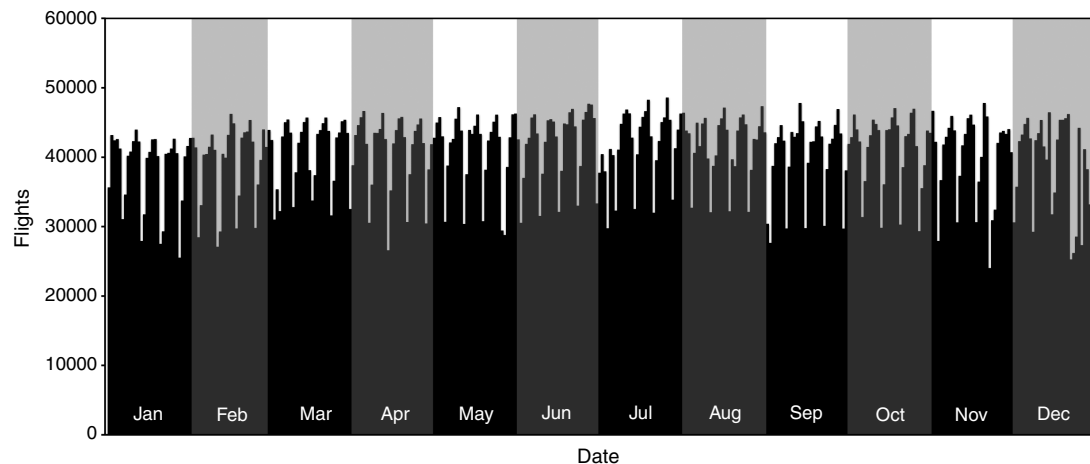


Fig. 3 Daily traffic count variations of 365 days in 2005–2007.

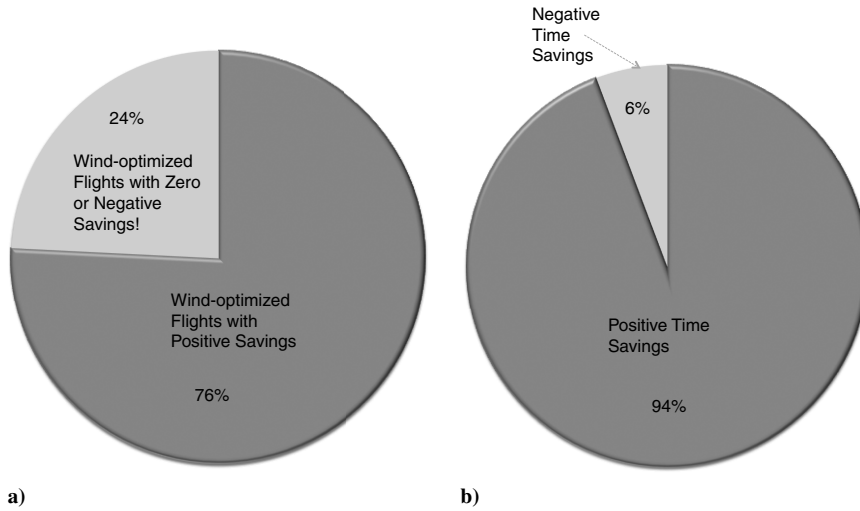


Fig. 4 Daily breakdown by flights and minutes.

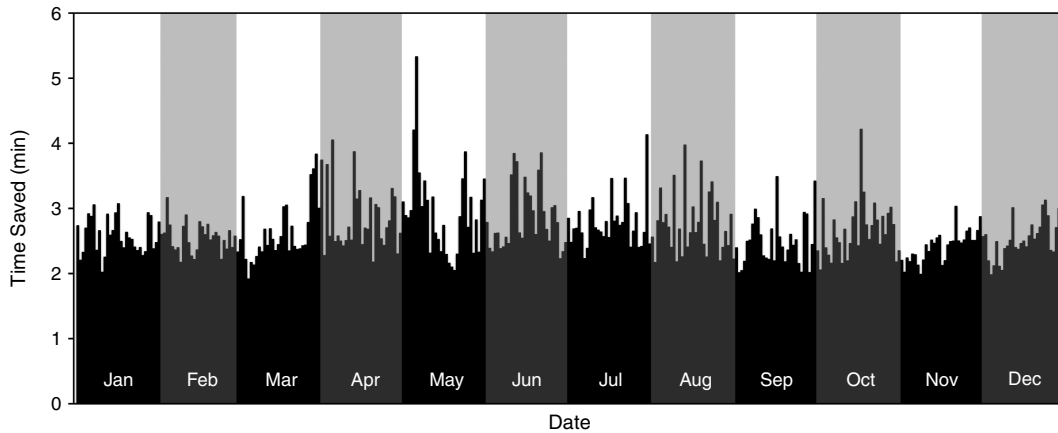


Fig. 5 Daily average en route time savings, per flight (minutes).

and days from 2006 and 2005 for which data was available were substituted. The substitutions were made on a day of the week basis, rather than by calendar date. For example, Tuesday, 16 May 2006, was substituted for Tuesday, 15 May 2007. This substitution method was selected to better preserve weekly traffic periodicity, as depicted later in this section. Among 365 days, 165 days are directly from 2007, 139 days are from 2006, and 61 days are from 2005. The results show the range of time and fuel savings, sector loading, conflict counts, and airport arrival rates throughout the simulated year.

**A. Time and Fuel Savings**

An average of 40,493 flights were simulated per day. Roughly 63% of flights, being shorter than 500 n mile or cruising at less than 18,000 ft, are not wind-optimized and are excluded from time and fuel-saving calculations. Traffic counts throughout the simulated year were fairly steady, with a slight decrease in traffic during the winter months, as shown in Fig. 3.

In total, 14,780,004 flights were simulated, including 5,406,777 flights on wind-optimal routes. Out of these optimized flights,

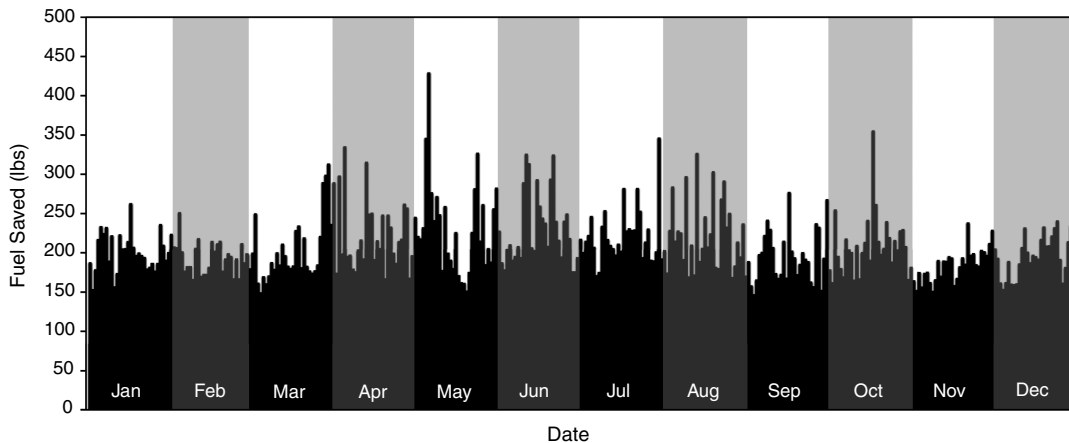


Fig. 6 Daily average fuel savings per flight (pounds).

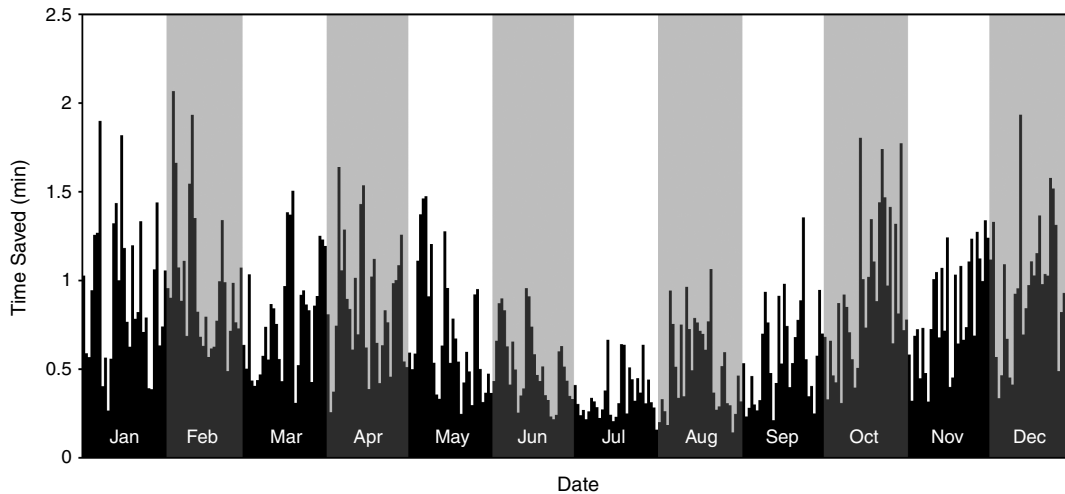


Fig. 7 Daily average time savings due to wind optimization, per flight (minutes).

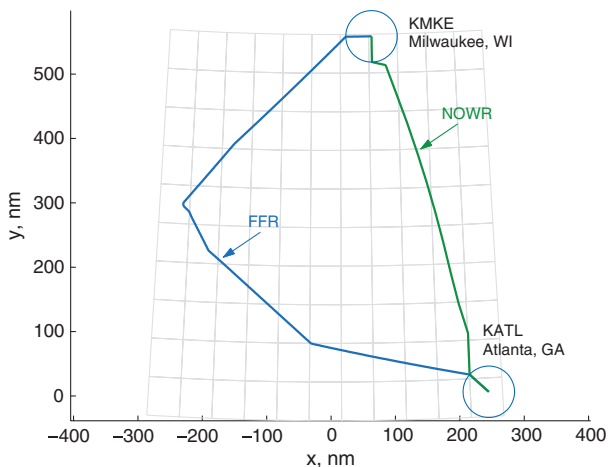


Fig. 8 Flight SKW3874 from KMKE to KATL: FFR is in blue on the left, NOWR is in green on the right.

4,097,457 had time and fuel savings. On average, 14,813 flights were optimized per day, and 11,226 (or around 76%) realized time and fuel savings. These values are depicted in Fig. 4a.

Negative savings result from the NOWR algorithm generating wind-optimal routes by examining the wind gradient solely along the

great-circle route. Since the assumptions underlying the NOWR algorithm are only valid for small perturbations from a locally optimum solution, as described in [14], flights can be routed into unfavorable wind fields if the route significantly deviates from the great circle. In the worst case, time saving from both distance and wind is negative for NOWR. Although 24% may seem high in terms of the number of flights shown in Fig. 4a, the negative total time saving is relatively low at 6%, as shown in Fig. 4b. On average, positive saving is 3.8 min per flight and negative saving is 0.7 min per flight.

Among flights that were optimized, average time and fuel savings realized were 2.7 min and 210 lb per flight. Daily average time and fuel savings per flight are shown in Figs. 5 and 6, respectively. These plots do not show a significant seasonal trend, but do demonstrate that wind-optimized routes realize consistent time and fuel benefits throughout the year. However, wind-optimal routes used in this experiment are, on average, 13.5 n mile shorter than their FFR counterparts. Time savings due solely to wind are separated from time savings due solely to distance by the method detailed in Appendix A. Examining only the wind time savings, flights realize an average time savings of 0.76 min per flight. Daily average wind time savings per flight are plotted in Fig. 7. A significant seasonal trend can be seen in this figure, with much smaller benefits occurring in the summer. This is consistent with the behavior of the jet stream, which is less pronounced in the National Airspace System during the summer months and is consistent with the maximum wind speed data shown in Fig. 2, where stronger wind occurs in the winter period.

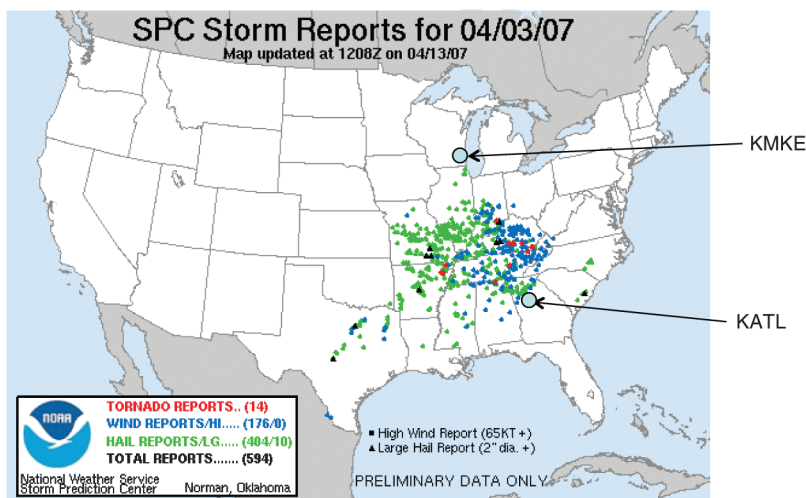
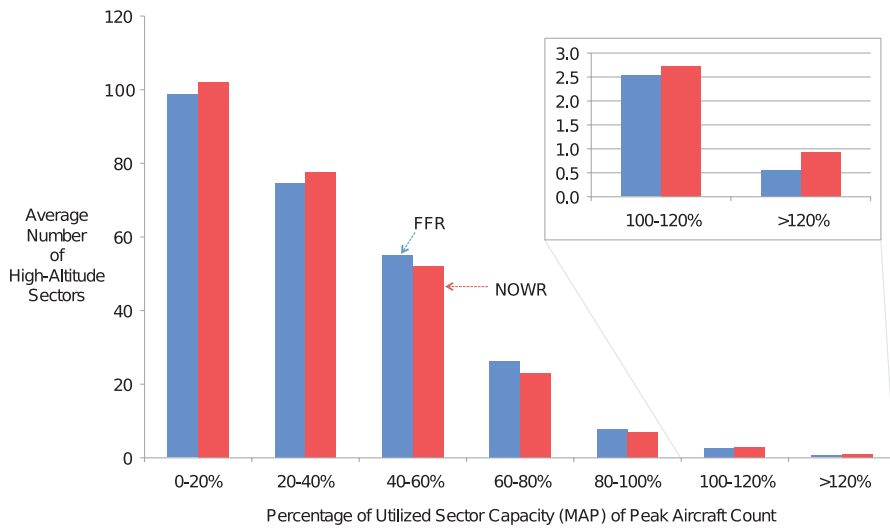


Fig. 9 Convective weather activities on 3 April 2007.

**Table 1 Top 10 sectors where NOWR's overloaded duration is largest compared to FFR**

| Sector | MAP value | Additional overloaded duration of NOWR |         |
|--------|-----------|--|---------|
|        |           | Hours/day                              | Percent |
| ZTL50  | 13        | 5.2                                    | 22      |
| ZNY75  | 15        | 3.8                                    | 16      |
| ZFW93  | 18        | 2.9                                    | 12      |
| ZMP12  | 18        | 2.9                                    | 12      |
| ZDC37  | 12        | 2.8                                    | 12      |
| ZLA37  | 15        | 2.6                                    | 11      |
| ZHU26  | 14        | 2.3                                    | 10      |
| ZMA02  | 20        | 1.7                                    | 7       |
| ZAU45  | 13        | 1.4                                    | 6       |
| ZNY73  | 14        | 1.3                                    | 5       |

Savings numbers that do not distinguish wind time savings from time savings due to distance do not account for certain real-world conditions that may prevent wind-optimal routes from being flown. Some flights incur time and fuel savings that are unrealistically large, due to significant deviations in the FFR, usually around convective weather or special-use airspace. Wind-optimized routes do not include these deviations, so some NOWR flights fly much shorter distances, and correspondingly report very large savings, compared to FFR. As an example, SkyWest flight SKW3874, departing General Mitchell International Airport in Milwaukee, Wisconsin, on 3 April 2007, maneuvered widely around convective weather activity on its way to Hartsfield-Jackson Atlanta International Airport. The flight's NOWR counterpart, ignorant of weather conditions, took a much more direct route. This resulted in presumptive time and fuel savings of almost 40%. The two flight routes are presented in Fig. 8, and a map of the convective weather activity on 3 April 2007 is presented in Fig. 9. In Fig. 8, the track on the left corresponds to the FFR route and the track to the right corresponds to the NOWR route.



**Fig. 10 Average number of high-altitude sectors vs used sector capacity.**

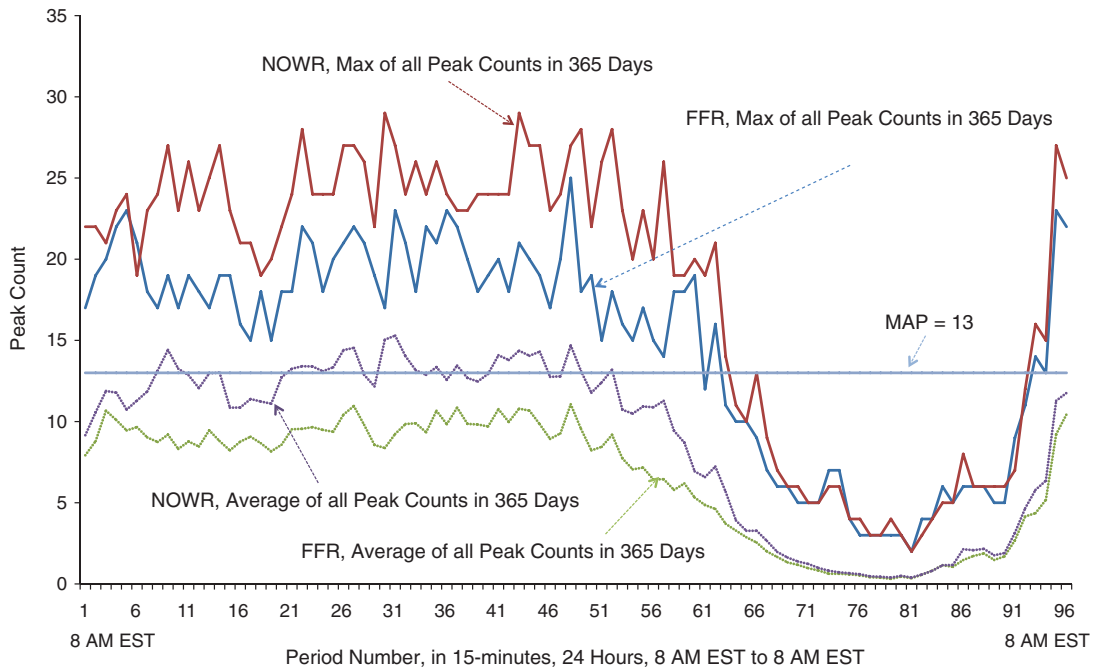


**Fig. 11 Maximum and average of peak counts in ZTL50 for an average day (96 15-minute bins).**

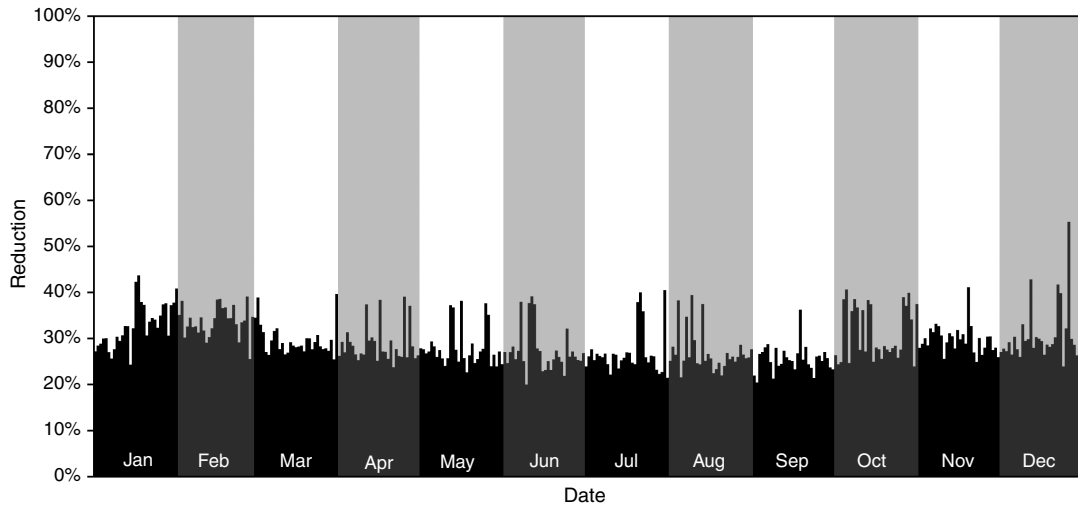


Fig. 12 Reduction in average conflict counts.

**B. Sector Loading**

Sector loading is studied by examining the time duration when the aircraft count is over the MAP value. Average time durations are calculated for each sector by adding the time duration that the sector’s aircraft count is over the MAP value for each day and dividing the sum by 365. Table 1 lists the top 10 sectors in terms of the highest difference of these time durations between FFR and NOWR. The top sector ZTL50 spent only 2.3 h per day above MAP in the FFR case, but 7.5 h in the NOWR case, a difference of 5.2 h per day.

Figure 10 shows average-day histograms of high-altitude sectors against sector loading with respect to their respective MAP values (NOWR in red and FFR in blue). The vertical axis shows the number of high-altitude sectors and the horizontal axis shows the percent capacity bins with respect to MAP values. When NOWR loading is at 100% and above, the average number of overcapacity sectors in any 15 min period is less than four. This small difference is shown in the zoomed-in portion to the right, by adding the counts of the two red bars. The difference in sector loading between NOWR and FFR is even smaller. It is less than one sector at any 15 min period at a time.

Finally, Fig. 11 shows the sector loading differences between NOWR and FFR for the worst performing sector, ZTL50, as listed in Table 1 before. This sector has the highest overload above the MAP values. This figure shows the maximum and average curves corresponding to an average-day peak count on the vertical axis and 96 15-minute bins a day on the horizontal axis. The minimum curves

are not shown to reduce clutter, but both curves lie below the MAP value.

The curves in this figure are generated as follows. For the maximums, in each 15 min period of a day, its peak count is compared to all other peak counts of the same period from the rest of the 365 days. The highest count corresponds to a point for the period on the maximum curve. The peak counts from all 96 bins form a maximum load curve for the sector. The same procedure is used to generate the minimum peak count curves and average peak count curves. This figure shows the worst-case sector load variation of flying wind-optimal routes. At the largest difference between the maximum curves, NOWR has 12 flights more than FFR. On average, NOWR is worse than FFR by 3.5 flights. Issues such as this would need to be addressed in other studies, like those done in the dynamic sectorization area before wind-optimal routes would be allowed. NASA has ongoing programs studying dynamic airspace configuration based on congestion and flow patterns.

**C. Conflicts**

Peak and average values of instantaneous conflict counts were used to gain insight of the air traffic controller workload. A lower number of conflicts were observed in the NOWR cases, as expected from their more distributed routes away from fixed routes such as jetways. Daily peak conflict counts decreased, on average, by about

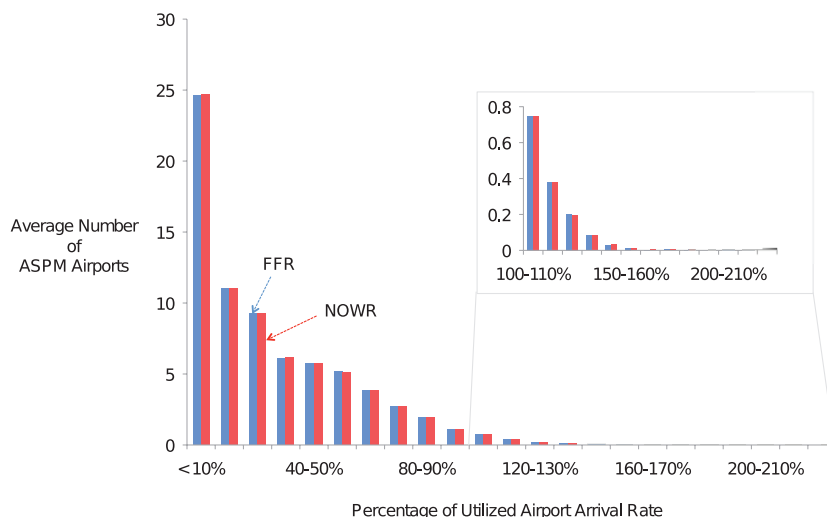


Fig. 13 Average number of ASPM airports vs used airport arrival rates.

**Table 2 Top eight ASPM airports where overloaded time duration of NOWR is longer than FFR**

| Airport  | Arrival capacity | Additional overloaded duration of NOWR |         |
|--|------------------|--|---------|
|  |                  | Minutes/day                            | Percent |
| KATL: Hartsfield-Jackson Atlanta International Airport | 96               | 6                                      | 0.40    |
| KORD: Chicago O'Hare International Airport             | 100              | 5                                      | 0.30    |
| KEWR: Newark International Airport                     | 48               | 3                                      | 0.20    |
| KSFO: San Francisco International Airport              | 32               | 2                                      | 0.10    |
| KHOU: Houston William P. Hobby Airport                 | 28               | 2                                      | 0.10    |
| KDTW: Detroit Metropolitan Wayne County Airport        | 72               | 1                                      | 0.10    |
| KRSW: Southwest Florida International Airport          | 18               | 1                                      | 0.10    |
| KTPA: Tampa International Airport                      | 35               | 1                                      | 0.10    |

29%. Figure 12 shows the percent reduction of the peak conflict count of NOWR compared to FFR.

**D. Arrival Rates**

Airport arrival rates remain approximately unchanged from FFR to NOWR operations. For each of the 365 simulated days, the peak hourly arrival rate was calculated for both the FFR and NOWR cases at each of the 73 ASPM airports in the continental United States. A histogram of these peak counts was created and then normalized by dividing by 365, so that, similar to the presentation of sector loading, the histogram can be regarded as the distribution of ASPM airports on an average day. No significant differences were observed between FFR and NOWR cases.

Airport arrivals as a percentage of published arrival capacities are also considered. The arrival capacities used in this paper are reported in [15]. For all 365 days, at the 73 ASPM airports, the hourly arrival rate is divided by the airport's arrival capacity at every hour; so 24 values are calculated per day for each airport. These values are averaged by number of days and hours to show the distribution of ASPM airports at any given hour. This histogram is displayed in Fig. 13, with blue columns representing the FFR case and red columns representing the NOWR case. The difference between the two cases is very small.

The airports where NOWR operation increased arrival loading are shown in Table 2. Atlanta is the most affected airport, and there are, on average, 6 min per day when arrival loading increased for the

**Table 3 Cost and benefit summary**

| Metric                                  | Cost and benefit  |
|---|---|
| Flight time                             | On average, NOWR saves 2.7 min per optimized flight per day.                |
| Fuel                                    | On average, NOWR saves 210 lb per optimized flight per day compared to FFR. |
| Sector loading in high-altitude sectors | No significant variation.   |
| Conflicts in class A airspace           | NOWR has an average of 29% fewer conflicts than FFR.                        |
| Arrival rate                            | No significant variation.   |

NOWR case. This is not considered to be a significant detriment to operations. Figure 14 depicts the average and maximum arrival rates for each hour of the day, and it is clear that arrivals do not change significantly under NOWR operation.

**VI. Conclusions**

An insight into benefits and cost variability is presented in support of flying wind-optimal routes. The time and fuel savings realizable through wind optimization have been well known, documented, and practiced for decades. This paper reinforces previous findings of savings with an extensive data set. From the results, except for a small

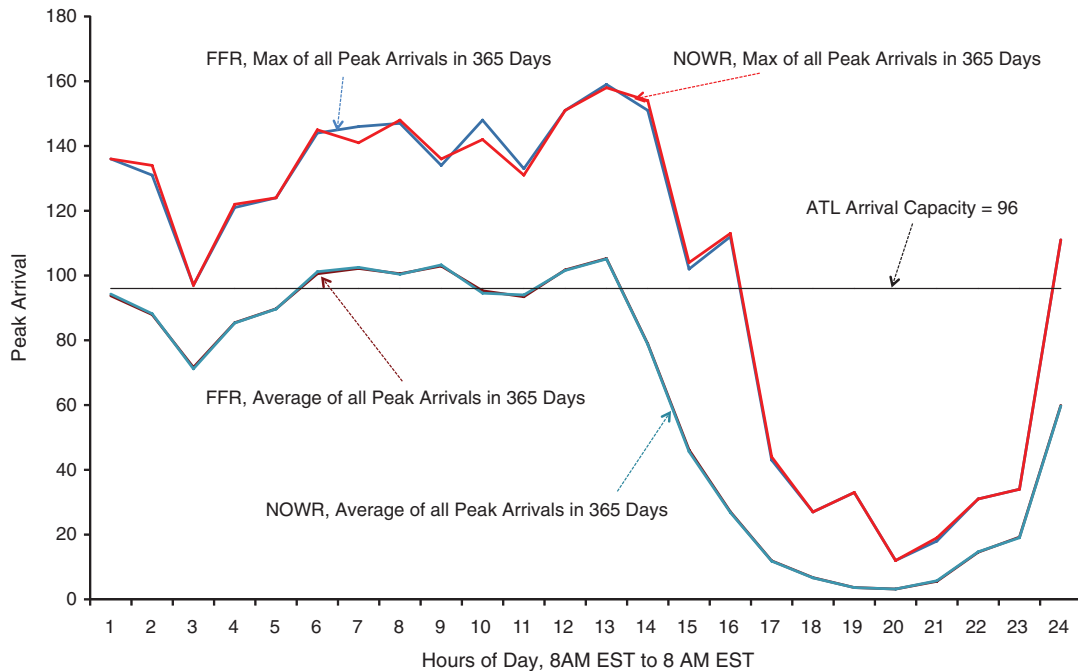


**Fig. 14 Maximum and average of peak arrival rates at KATL for an average day.**

number of cases with negative savings due to the approximation characteristics of the neighboring optimal wind routing algorithm, wind-optimal routes save, on average, 2.7 min in flight time and 210 lb of fuel per flight, while showing no significant cost variation. Conflicts in class A airspace are significantly reduced, as much as 29% on average, by the dispersion of flights from prescribed, structured routes. Airport arrival rates remain almost identical. Although a small number of sectors show considerably higher aircraft counts for the wind-optimal route on average, wind optimization causes, at most, one additional high-altitude sector to be overloaded. These results are summarized in Table 3.

### Appendix A: Types of Time Savings

FFR and NOWR differ in many ways. Since the FFRs have to take into account many factors such as jet route structures, nav aids, special-use airspaces, or weather, they tend to be indirect. NOWRs are also indirect in order to take maximum advantage of the wind. Since the two routes generally have different distances, it is difficult to directly compare the flight times. To mitigate the effect of distance variation, a speed-distance metric is devised.

If constant speeds are assumed, the relations between the speed, time, distance for FFR and NOWR are shown in Fig. A1 and Eqs. (A1) and (A2):

$$T_{\text{FFR}} = \frac{d_{\text{FFR}}}{V_{\text{FFR}}} \quad (\text{A1})$$

$$T_{\text{NOWR}} = \frac{d_{\text{NOWR}}}{V_{\text{NOWR}}} \quad (\text{A2})$$

Total time saving is the difference between the FFR flight time and NOWR flight time, as shown in Fig. A2 and Eq. (A3):

$$\Delta T = T_{\text{FFR}} - T_{\text{NOWR}} \quad (\text{A3})$$

Let  $T_1$  be the time that it takes an aircraft to fly the NOWR route with FFR speed:

$$T_1 = \frac{d_{\text{NOWR}}}{V_{\text{FFR}}} \quad (\text{A4})$$

The time difference between the  $T_{\text{FFR}}$  and  $T_1$  represents the time difference due to the distance difference, as denoted by  $T_d$  in Eq. (A5):

$$\Delta T_d = T_{\text{FFR}} - T_1 = T_{\text{FFR}} - \frac{d_{\text{NOWR}}}{V_{\text{FFR}}} = T_{\text{FFR}} \left( 1 - \frac{d_{\text{NOWR}}}{d_{\text{FFR}}} \right) \quad (\text{A5})$$

So, the time saving due to optimally using wind can be computed by subtracting the distance influence from the total time saving, as described in Eq. (A6):

$$\Delta T_w = \Delta T - \Delta T_d = T_{\text{FFR}} \frac{d_{\text{NOWR}}}{d_{\text{FFR}}} - T_{\text{NOWR}} \quad (\text{A6})$$

Since these metrics assume constant speed, they will not provide the exact breakdown between savings due to distance and savings due to wind. However, for relatively long-haul flights that have larger

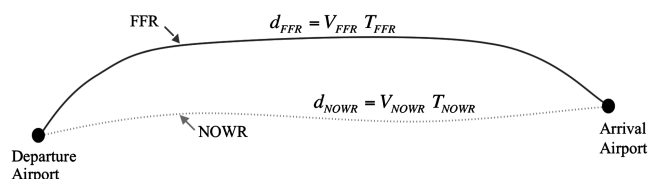


Fig. A1 FFR vs NOWR.

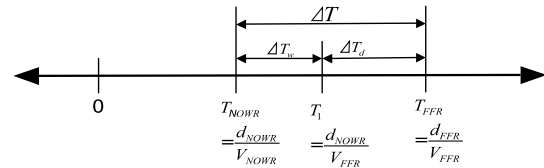


Fig. A2 Time-saving portions from wind vs from distance.

cruise portions, the constant speed assumption holds reasonably well. These metrics will provide a general idea of net time savings due to optimally using wind.

### Acknowledgments

The authors thank Gano Chatterji for his continuous support, encouragement, and valuable discussions. The authors also thank Jack Lai and Allen Goldberg for their postprocessing code and support. Finally, the authors thank Michael Downs and Shon Grabbe for reviewing the draft of this paper and providing valuable feedback that enhances its quality.

### References

- [1] Heimlich, J., *U.S. Airlines Operating in an Era of High Jet Fuel Prices*, Air Transport Association of America, Inc., Washington, D.C., 11 July 2007.
- [2] Chin, D. K., and Melone, F., "Using Airspace Simulation to Assess Environmental Improvements from Free Flight and CNS/ATM Enhancements," *Proceedings of the 1999 Winter Simulation Conference*, Vol. 2, Inst. of Electrical and Electronics Engineers, Piscataway, NJ, Dec. 1999, pp. 1295–1301. doi:10.1109/WSC.1999.816856
- [3] Barnett, A., "Air Safety: End of the Golden Age?" *Journal of the Operational Research Society*, Vol. 52, No. 8, Aug. 2001, pp. 849–854.
- [4] Grabbe, S., and Sridhar, B., "Central East Pacific Flight Routing," AIAA Guidance, Navigation, and Control Conference and Exhibit, Keystone, CO, AIAA Paper 2006-6773, 21–24 Aug. 2006.
- [5] Bilimoria, K. D., and Lee, H. Q., "Properties of Air Traffic Conflicts for Free and Structured Routing," AIAA Guidance, Navigation, and Control Conference and Exhibit, Montreal, AIAA Paper 2001-4051, 6–9 Aug. 2001.
- [6] Jardin, M. R., "Analytical Relationships Between Conflict Counts and Air-Traffic Density," *Journal of Guidance, Control, and Dynamics*, Vol. 28, No. 6, Nov.–Dec. 2005, pp. 1150–1156. doi:10.2514/1.12758
- [7] Palopo, K., Windhorst, R. D., Musaffar, B., and Refai, M., "Economic and Safety Impacts of Flight Routing in the National Airspace System," 7th AIAA Aviation Technology, Integration and Operations Conference (ATIO), Belfast, Northern Ireland, AIAA Paper 2007-7805, 18–20 Sept. 2007.
- [8] Datta, K., and Schultz, G., "An Evaluation of TAAM for Free Flight Modeling," *Final Report for Advanced Air Transportation Technology Program*, NASA Ames Research Center, Moffett Field, CA, Aug. 1996.
- [9] Jardin, M. R., and Bryson, A. E., Jr., "Neighboring Optimal Aircraft Guidance in Winds," *Journal of Guidance, Control, and Dynamics*, Vol. 24, No. 4, 2001, pp. 710–715. doi:10.2514/2.4798
- [10] Meyn, L., Windhorst, R. D., Roth, K., Van Drei, D., Kubat, G., Manikonda, V., et al., "Build 4 of the Airspace Concept Evaluation System," *AIAA Modeling and Simulation Technologies Conference and Exhibit*, Keystone, CO, AIAA, 21–24 Aug. 2006.
- [11] "Airline Operational Control Overview (U.S.)," FMS-ATM Next Generation (FANG) Team, Federal Aviation Administration, July 1997.
- [12] "User Manual for the Base of Aircraft Data (BADA) Revision 3.6," Eurocontrol Experimental Centre, Note No. 10/04, July 2004.
- [13] Peters, M., and Konyak, M. A., "The Engineering Analysis and Design of the Aircraft Dynamics Model for the FAA Target Generation Facility," Seagull Technology, Inc., Los Gatos, CA, Nov. 2003, pp. 43–45.
- [14] Jardin, M., "Toward Real-Time En Route Air Traffic Control Optimization," Ph.D. Dissertation, Dept. of Aeronautics and Astronautics, Stanford Univ., Stanford, CA, 2003.
- [15] Chatterji, G. B., and Zheng, Y., "Impact of Airport Capacity Constraints on National Airspace System Delays," *7th AIAA Aviation Technology, Integration and Operations Conference (ATIO)*, Belfast, Northern Ireland, AIAA Paper 2007-7712, 18–20 Sept. 2007.